ACS Sustainable Chemistry & Engineering

Research Article

pubs.acs.org/journal/ascecg

Solvent-Exfoliated and Functionalized Graphene with Assistance of Supercritical Carbon Dioxide

Lihua Li,[†] Xiaoli Zheng,[†] Jianjun Wang,[‡] Qiang Sun,[‡] and Qun Xu*,[†]

[†]College of Materials Science and Engineering, Zhengzhou University, Zhengzhou 450052, China

[‡]Center for Energy and Quantum Structures, College of Physics and Engineering, Zhengzhou University, Zhengzhou 450001, China

ABSTRACT: Graphite was successfully exfoliated into graphene by pyrene and another three derivatives (1-pyrenecarboxylic acid (PCA), 1-pyrenebutyric acid (PBA), and 1-pyrenamine (PA)) with the assistance of supercritical carbon dioxide (SC CO_2) in this work. The resulting graphene was characterized by transmission electron microscopy (TEM), Fourier transform infrared spectroscopy (FTIR), Raman spectra, and fluorescence spectra. High-quality and noncovalent functionalized single or few layer graphene were obtained. van der Waals corrected first-principles approach within density functional theory (vdW-DFT2) was used to investigate the interaction energy of different pyrene-derivatives on graphene and inside the two graphene. The results showed that pyrene and pyrene-derivatives can act as a "molecular wedge" to exfoliate graphene from graphite well. A further graphene/gold nanoparticle composite was also successfully obtained, which indicates that pyrene-derivatives firmly adsorbed on the surface of graphene can act as the interlinkers between graphene and Au NPs or other rare metal nanoparticles. Therefore, the functionalized graphene with different pyrene-derivatives will have potential applications in nanofunctional materials, nanoreactor devices, and catalysis fields.

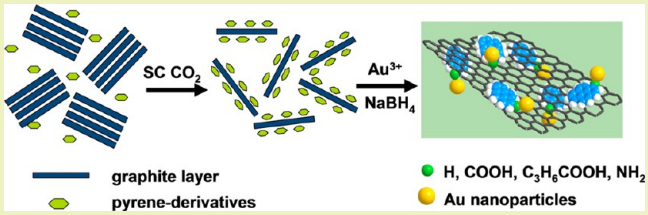

KEYWORDS: *Graphene, Pyrene Derivatives, Supercritical CO_2, Density Functional Theory*

INTRODUCTION

Graphene is a monolayer of aromatic carbon atoms arranged in a honeycomb network,[1,2] and this unique structure endows graphene with marvelous mechanical, electrical, and thermal proprieties.[3−6] For its further application, an efficient approach to produce graphene in large quantities is urgently required.[7−10] Among the reported methods, liquid-phase exfoliation has shown great advantages for bulk production of graphene sheets.[11] It mainly involves liquid-phase exfoliation from graphite oxide[12] and pristine graphite.[13] Graphite oxide can be easily exfoliated into monolayer graphene oxide (GO) and form stable colloid suspension in water or organic solvent with sonication. However, the oxidization process introduces many irreversible defects and destroys the rigid properties of graphene.[14] The use of pristine graphite as the starting material is an excellent alternative. In addition, the graphene produced by this method can be conveniently functionalized and deposited on any substrate with simple processing.

Functionalization of graphene has been considered as an efficient way to improve the dispersibility and stability.[15,16] Noncovalent functionalization of graphene that is attached the molecular to the surface of graphene through $\pi-\pi$ interaction or van der Waals forces shows great advantage without disrupting the structure, and it preserves the intrinsic properties.[17−19] Surfactant, polymer, and amphipathic aromatic molecular have been widely used as stabilizer. Among the various modifiers, pyrene-derivatives show the distinct advantage. They can act as nanographene to repair the possible defects in the graphene flakes under thermal treatment[20] and electrical "glue" soldering vicinal graphene flakes to reduce the contact resistance between graphene.[21] Recently, some research work reported that pyrene-derivatives could intercalate and exfoliate graphite into graphene.[21,22] Nevertheless, the theory of graphene exfoliation mechanism using different pyrene-derivatives has not been well established. It is necessary to study the interaction between the different pyrene-derivatives and graphene via experimental results and theoretical simulation.

Graphite intercalation compounds (GICs) have been widely used as staring materials for graphene production.[23−25] However, the conventional method for the intercalants fully inserting into the graphite layer is time-consuming.[23] Supercritical fluids (SCFs), which possess "gas-like" diffusivity, "liquid-like" density, low viscosity, and zero surface tension, show better transport properties than conventional organic solvent.[26] These features make SCFs the superior solvents for rapid penetration and intercalation of the layered structure to reduce the duration of time.[27] In addition, SCF is an environmental friendly technique, especially considering the scale-up preparation of graphene in the future, green chemistry and sustainable process is necessary. Supercritical carbon dioxide (SC CO_2) has been widely studied because of its easily accessible supercritical conditions, low toxicity and low costy.[28] It has been utilized to intercalate and exfoliate layered materials, such as graphite and clay.[26,28−30] The excellent solubility of pyrene-derivatives in CO_2 or their good

Received: July 28, 2012
Revised: September 16, 2012
Published: October 9, 2012

compatibility with CO_2[31,32] make the pyrene-derivatives can be used as a kind of suitable additives to cleave the graphite.

In this work, we choose pyrene and another three pyrene-derivatives (1-pyrenecarboxylic acid (PCA), 1-pyrenebutyric acid (PBA) and 1-pyrenamine (PA)) and study their effect on the exfoliation of graphite with assistance of SC CO_2. High-quality and noncovalent functionalized single or few layer graphene sheets were successfully obtained in all cases. In addition, we used van der Waals corrected first-principles approach within density functional theory (vdW-DFT2) calculations to identify the experimental results. The results of the theoretical modulation better illustrate the experimental phenomena. Further nanocomposite of gold nanoparticles (Au NPs) modified on the pyrene-derivatives exfoliate graphene was obtained. And it indicates again the successful exfoliation and modification of graphene can be achieved in one step.

EXPERIMENTAL SECTION

Materials. Graphene powder was purchased from Acros Organics (Catalog 385031000). Pyrene (98%) and 1-pyrenebutyric acid (PBA) (97%) were bought from J & K Scientific Ltd. (China). 1-Pyrenecarboxylic acid (PCA) (98%) and 1-pyrenamine (PA) (>98%) were purchased from Tokyo chemical industry Co., Ltd. (Japan). D-Dimethylformamide (DMF) and sodium borohydride ($NaBH_4$) were supplied by Guangdong guanghua Sci-Tech Co., Ltd. (China). $HAuCl_4$ was purchased from Aldrich. Trisodium citrate was purchased from Sinopharm Chemical Reagent Co., Ltd. (China). All reagents were used as received.

Preparation of Noncovalent Functionalized Graphene Sheets. In a typical experiment, graphite powder (20 mg) and pyrene-derivatives (0.013 mmol) were dispersed in DMF (10 mL) by low-power sonication for 3h. Then, the mixture was transported to a preheated (40 °C) stainless steel reactor (50 mL) and CO_2 was charged into the reactor to desired pressure (16 MPa). The mixture was stirred in the SC CO_2 for 6 h. The reaction was terminated by rapid depressurization of the vessel. The sample was centrifuged and washed with ethanol to remove the free pyrene-derivatives. The sediment was redispersed in DMF. The solution was then sonicated for an additional two hours resulting in a stable dispersion, followed by centrifuged for 20 min at 1000 rpm. The top half of the supernatant was piped off for characterization.

Fabrication of Graphene/Gold Nanopraticles Composites. The method for fabricating graphene/gold nanoparticles composite was inspired by a previously described method for preparing gold seeds.[33] The graphene was isolated from the DMF by centrifugation (9000 rpm, 15 min) and then redispersed in 9.8 mL of aqueous solution containing 5.0×10^{-4} M $HAuCl_4$. Trisodium citrate solution (0.2 mL, 0.025 M) was added to the solution and stirred for 3 min. At the same time, 10 mL of 0.01 M $NaBH_4$ solution was prepared by adding $NaBH_4$ to 10 mL of ice-cold 0.025 M trisodium citrate solution. Then, 0.6 mL of $NaBH_4$ solution was added to the solution with vigorous stirring. The solution turned purple immediately, indicating the formation of gold particles. The mixture solution was stirred another 10 min and set for 2 h. Finally, the resulting product was collected by centrifugation, washed by ethanol for three times, and then dispersed in 1 mL of ethanol.

Characterization. Transmission electron microscopy (TEM) was performed using a FEI Tecnai G^2 20 and holey carbon grid with an accelerating voltage of 200 kV. Atomic force microscopy (AFM) was performed using a SPM-9500J3. The sample was prepared by drop casting the dispersion onto SiO_2/Si substrate. Raman spectra were obtained at 532 nm with a Renishaw invia Raman Microscope using a 50× objective lens at room temperature. The samples were prepared by drop casting a few drops of the dispersion onto glass slide. FT-IR spectra were measured using a BRUKE TENSOR27 instrument. KBr was used to prepare sample pellets. UV−vis absorption spectral measurements were carried out with a Shimadzu UV-240/PC spectrophotometer. Fluorescence spectra were recorded using a Deinburgh FL/FS TCSPC 920 spectrofluorophotometer.

Models and Computational Details. All the calculations were performed by the VASP code[34] using the projector augmented-wave (PAW) method for describing ion-electron interaction.[35] The exchange-correlation interaction was treated in the GGA in the parametrization of Perdew, Burke, and Ernzerhof (PBE).[36] Long-range dispersion corrections have been taken into account within a DFT-D2 approach of Grimme, as implemented by Bucko et al.[37] Standard values for the dispersion coefficient of C_6 (1.75, 0.14 and 0.7), vdW radii (1.452, 1.001 and 1.342) of carbon, hydrogen, and oxygen atoms have been used, respectively. The wave function was expanded in a plane-wave basis with an energy cutoff of 480 eV. The irreducible Brillouin-Zone integration was carried out by using the $19 \times 19 \times 1$ and $1 \times 1 \times 1$ Monkhorst−Pack grids for the 1×1 and 7×7 graphene supercells.[38] The total energy was converged up to 10^{-4} eV for the electronic structure relaxations. And for geometry optimizations, all the internal coordinates were relaxed until the Hellmann−Feynman forces were less than 0.02 eV/Å. A vacuum layer of ∼15 Å was set to avoid the interactions between the adjacent images for all calculated systems.

RESULT AND DISCUSSION

Preparation of Pyrene-Derivatives Modified Graphene Sheets with Assistance of SC CO_2. The process of exfoliation and modification of graphene using pyrene-derivatives with assistance of SC CO_2 is schematically illustrated in Scheme 1.

Scheme 1. Schematic Illustration of Exfoliation and Modification of Graphene Using Pyrene-Derivatives with Assistance of SC CO_2

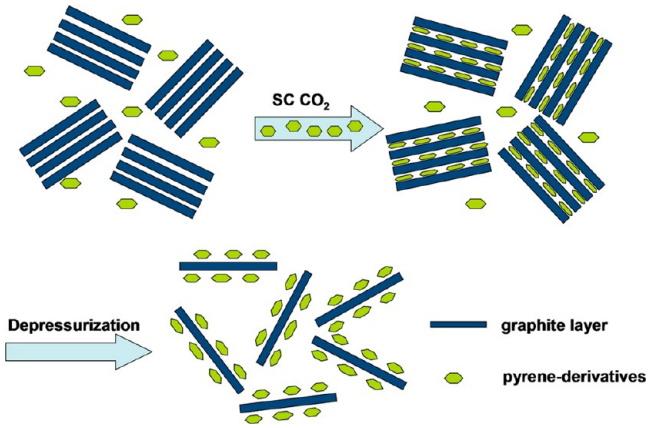

First, graphite and pyrene-derivatives are dispersed in dimethylformamide (DMF) by bath sonication. Then carbon dioxide is injected to the reaction system and maintained above its critical temperature and critical pressure. Under the supercritical fluid experimental condition, the soluble pyrene-derivatives therein can be carried into the interlayer of graphite. At the same time, the graphite layers are pushed apart with the expansion of the SC CO_2. With the release of CO_2, the pyrene-derivatives precipitate and adsorb on the surface of graphene layers because of the $\pi-\pi$ interaction.[18,39] And the noncovalent functionalized graphene that can be well-dispersed in solvent is obtained.

Here, we utilized pyrene, PCA, PBA, and PA to exfoliate and modify graphene. After careful removal of free pyrene-derivatives and any unexfoliated graphite microparticles, the dispersion of pyrene-derivatives modified graphene (G-pyrene, G-PCA, G-PBA, and G-PA) obtained was transferred onto holey carbon grids and subjected to transmission electron microscope (TEM) analysis. As shown in Figure 1, monolayer or few layer graphene can be prepared by this method. Figure 1b and c show disordered

dx.doi.org/10.1021/sc3000724 | ACS Sustainable Chem. Eng. 2013, 1, 144−151

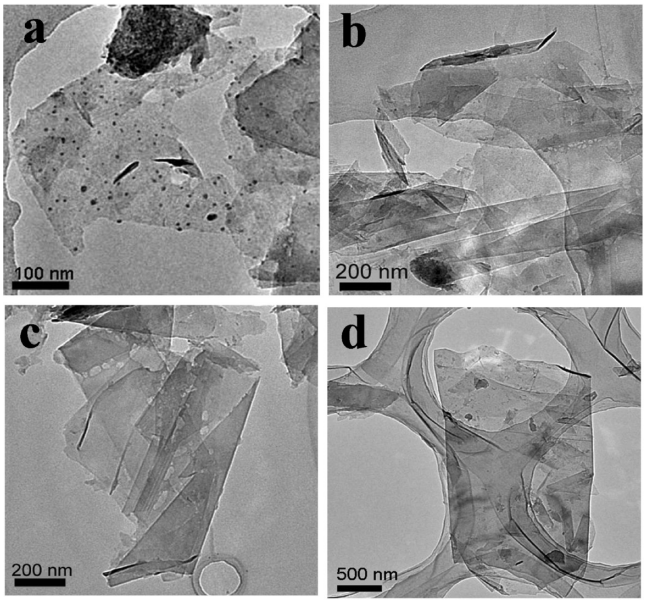

Figure 1. TEM images of graphene sheets: (a) G-pyrene, (b) G-PCA, (c) G-PBA, and (d) G-PA.

multilayer with folded edges. A large thin flake with lateral dimensions about several micrometers highly scrolled shows in Figure 1d. And in Figure 1 a many aggregates are observed on the surface of graphene, indicating that there are still remaining pyrene-derivatives functionalized on graphene due to robust $\pi-\pi$ interaction even after repeating centrifuged washing. The TEM images reveal that graphite is successfully exfoliated by pyrene-derivatives. And it can be further indicated by the following experiments using Au nanoparticles to modify the obtained graphene.

Atomic force microscope (AFM) was used to measure the thickness of the exfoliated graphene sheets. Figure 2a is the typical AFM image of PA-G flakes deposited on SiO_2/Si substrates. The thickness of single-layer graphene is fall in a range of 1.1−1.5 nm which is consistent with the thickness obtained by other groups reported previously.[27,39] Height profiles taken along the black lines 1 and 2 in Figure 2a, indicating that the sheets of 1 correspond to single-layer graphene and that of 2 to bilayer graphene, respectively. In addition, statistical analysis was used to provide further information on the efficiency of graphite exfoliation. Figure 2b is the histogram of layer number distribution obtained by analysis the thickness of 100 pieces of graphene sheets through AFM measurement. The sample is mainly composed of 1−3 layer graphene (82%), and the amount of single-layer graphene can reach 6%. The result of AFM further confirmed the effective of graphite exfoliation by our methods.

Raman spectroscopy is a powerful tool for indentifying the number of layers and structure defects of graphene.[40−42] The Raman samples were prepared by dropping a few drops of obtained graphene dispersion on a glass slide and recorded with green (532 nm) laser radiation. Figure 3 is the Raman spectra of graphite and graphene, there are three main features of all samples, D (~1350), G (~1580), and 2D (~2700) graphitic bands. The shape and position of 2D band are very sensitive to the number of graphene layers. As shown in Figure 2, the 2D

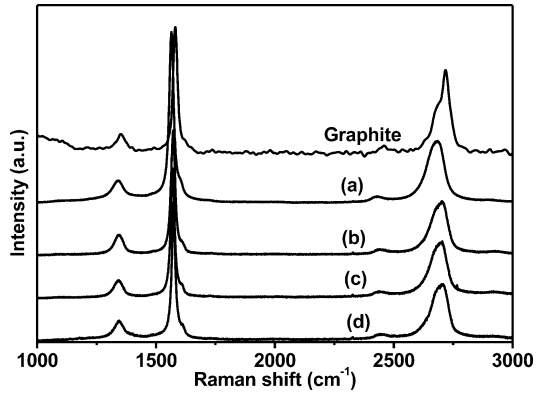

Figure 3. Raman spectra of graphite, (a) G-pyrene, (b) G-PCA, (c) G-PBA, and (d) G-PA.

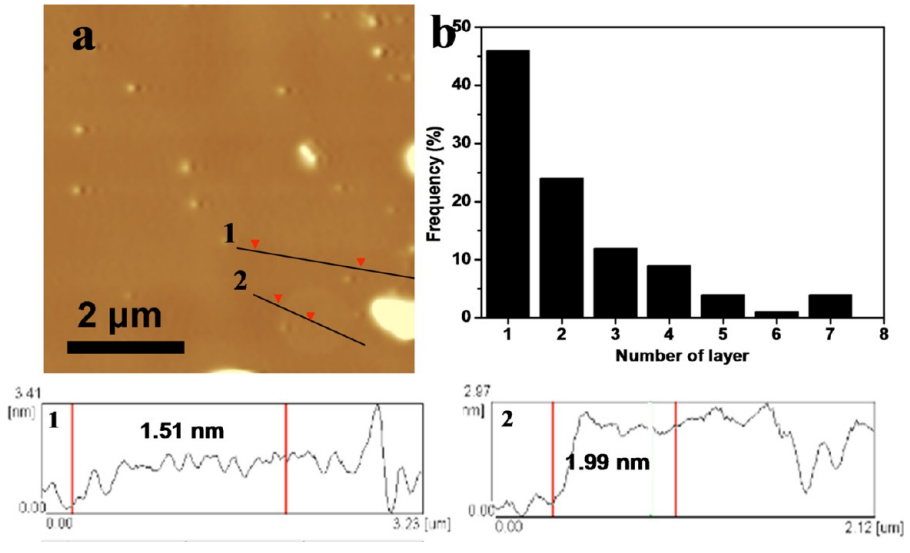

Figure 2. (a) Typical AFM image of G-PA flakes deposited onto SiO_2/Si substrates. Line profiles taken along the black lines 1 and 2, respectively, indicating that the sheets of 1 correspond to single-layer graphene and that of 2 to bilayer graphene. (b) Histogram of the distribution of layer number from the AFM measurement.

dx.doi.org/10.1021/sc3000724 | ACS Sustainable Chem. Eng. 2013, 1, 144−151

band in bulk graphite consists of two components and locates at 2718 cm^{-1}. The wavenumber of the 2D band of G-pyrene, G-PCA, G-PBA, and G-PA is 33, 14, 14, and 11 cm^{-1} lower than that of the graphite, respectively. The changes of 2D band between graphite and G-pyrene, G-PCA, G-PBA, and G-PA confirmed the efficient exfoliation of graphene.[40,43]

The peak at ~1350 cm^{-1} (D band) depends on the breathing mode of the 6-fold aromatic rings. It derives from disorders at edges or defects in samples. The intensity of the D-band reflects the defects level of the sample. From the Raman spectra of graphite, we can observe a small D band, which indicates small defect exist in the staring materials. After treatment, there are no obvious changes in D bands, the ratios of I_D/I_G for G-pyrene, G-PCA, G-PBA, and G-PA are calculated to be 0.15, 0.24, 0.20, and 0.21, respectively. They are comparable with the raw graphite (0.18) and much lower than the reduced graphene from GO (1.10).[44] The results of Raman indicate that the obtained graphene sheets are pretty ideal in property and it can be attributed to the high-diffusivity, low viscosity of SC CO_2, and short sonication processing. In addition, we compared the FTIR spectra of graphite and graphene, as shown in Figure 4. For

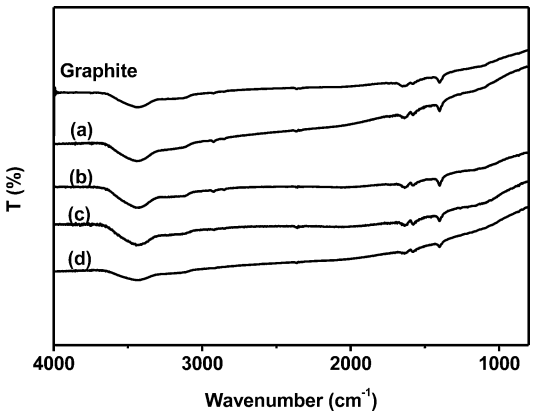

Figure 4. FT-IR spectra of graphite and graphene obtained after treatment with different pyrene-derivatives: (a) G-pyrene, (b) G-PCA, (c) G-PBA, and (d) G-PA.

graphene, the peaks appear for O−H stretching (3400 cm^{-1}), aromatic C═C stretching (1637, 1577 cm^{-1}) and O−H deformation (1400 cm^{-1}),[45,46] which is same as the raw graphite. It indicated again the pristine structure of graphene.

From the above discussion, we can conclude that graphite has been successfully exfoliated into mono- or few- layers graphene sheet using pyrene-derivatives with assistance of SC CO_2. In the following study, the dispersion of graphene was investigated via UV−vis absorption spectra and fluorescence spectra analysis. After removal of the free pyrene-derivatives by centrifugal washing, absorption spectra of the resulting graphene dispersions were characterized by UV−vis spectrophotometer. Figure 5 shows the UV absorption spectra of pyrene-derivatives, graphene, and graphene dispersions obtained. The graphene (dash line) exhibits one absorption band at 268 nm, which attribute to the electronic $\pi-\pi^*$ transition of the C═C bond. For pyrene-derivatives (dot line), there is one strong absorption band in the region of 300−400 nm, the absorption band near 336, 353, 343, and 413 nm originate from the pyrene, PCA, PBA, and PA, respectively. For the resulting graphene dispersions (solid line), it exhibits two absorption bands, one is a strong band around 268 nm because of the contribution of graphene and the other is a weak band at the range of 300−400 nm coming from the contribution of relevant pyrene-derivatives. The UV absorption spectra clear show the formation of functionalized graphene with different pyrene-derivatives on the graphene flakes.[18,39] To further study the interaction between pyrene-derivatives and graphene. We compared the fluorescence spectra of pyrene-derivatives and the obtained graphene dispersions in Figure 6. The fluorescence spectra of pyrene-derivatives show intense fluorescence with emission maxima at different region. However, in the case of obtained graphene dispersion the fluorescence intensity were extensively quenched, suggesting an effective electron or energy transfer between pyrene-derivatives and graphene.[16] The fluorescence spectra provide compelling evidence for the strong $\pi-\pi$ interaction between pyrene-derivatives and graphene.

As discussed above, we obtained high-quality noncovalent functionalized graphene by direct exfoliation of graphite using pyrene-derivatives with assistance of SC CO_2. In the following study, we employed computational simulations to identify the effect of pyrene and its derivatives.

Computational Simulations Based on the vdW-Refined DFT. All the calculation results were based on the van der Waals corrected first-principles approach within density functional theory (vdW-DFT2). The vdW-DFT2 calculations show that the interlayer binding energy between graphenes for AB stack is 50 meV per carbon atom with balance interlayer distance (3.25 Å), which is in good agreement with experimental result (52 ± 5 meV per carbon atom).[47] The optimized adsorption structure configurations between graphene and pyrene, PA, PCA, and PBA for hollow sites are shown in Figures 7 and 8. The structures of adsorption system changed slightly, and the dangling groups tend to be plane to adapt the adsorption system. The equilibrium adsorption distances have a slight difference near 3.3 Å for the four different molecules.

The adsorption energies for these systems are presented in Table 1, and ploted in Figure 9. As seen, pyrene and its derivatives have larger interaction energies than that of graphene dimers. This demonstrates that pyrene and its derivatives can easily bond to graphene than that of graphene on graphene by either AA or AB stacking. In addition, it should be noted that the addition of the dangling chains increases the interaction energy (in absolute values). The difference of interaction energy between the PBA/graphene and graphene dimers is as high as 21.4 meV $atom^{-1}$. The interaction energies of molecules inside two graphene sheets are more than two times as that of molecules on single-layer graphene (Table 1 and Figure 9), indicating that the molecules tend to insert the interlayer of graphite.

The nanofriction for pyrene, PCA, and PA on graphene have also been calculated. The comparisons of coefficients of friction with the different molecules show that all the above systems has lower friction coefficients than that of graphene on graphene under the same loads (Figure 10). This illustrates that pyrene, PCA and PA molecules can move easily between two graphene. In addition, the system of PCA on graphene has the smallest coefficient of friction, which means that pyrene-derivatives with proper dangling chains slid easier than pyrene on graphene. And the dangling chain is also an important factor in obtaining a homogeneous suspension of graphene. The large adsorption energy and low coefficient of friction of pyrene and its derivatives demonstrate that they can act as "molecular wedge" to exfoliate graphite to graphene.

Nanocomposite of Graphene/Gold Nanoparticles (Au NPs). Graphene is an ideal candidate for nanocomposite because

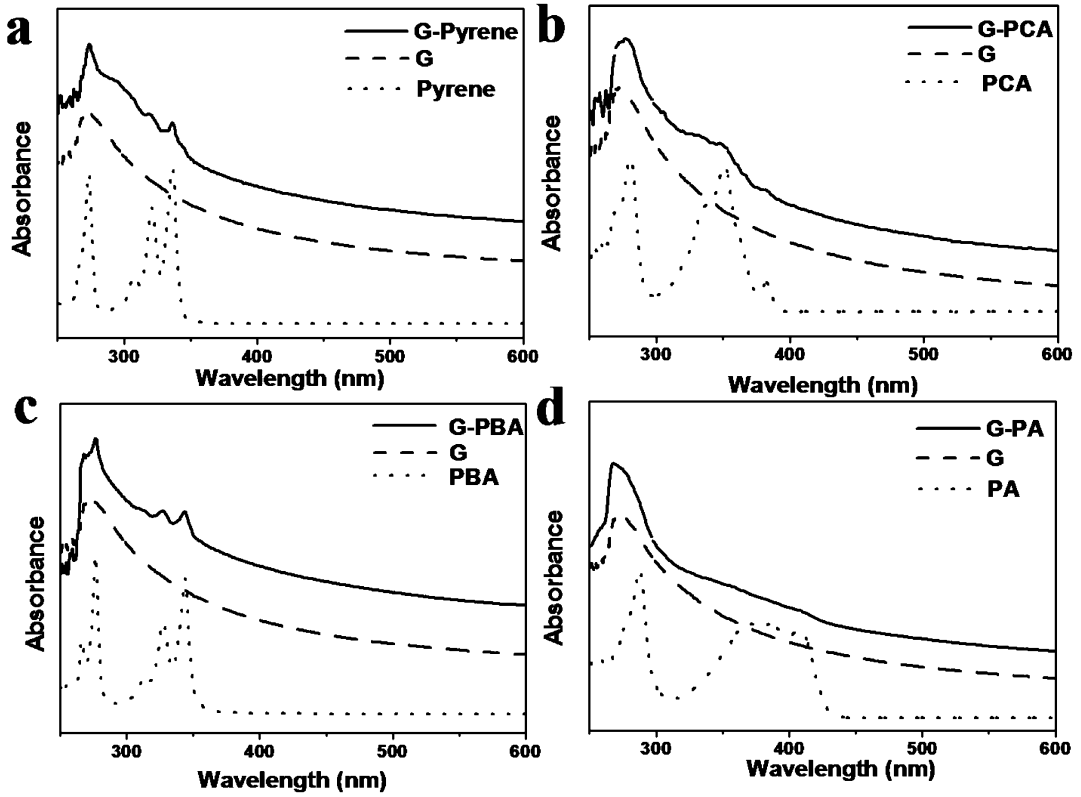

Figure 5. UV−vis spectra of Pyrene-derivatives and the relevant graphene dispersion: (a) G-pyrene, (b) G-PCA, (c) G-PBA, and (d) G-PA. UV−vis spectra of graphene without any pyrene-derivative modified was also shown here (dash line).

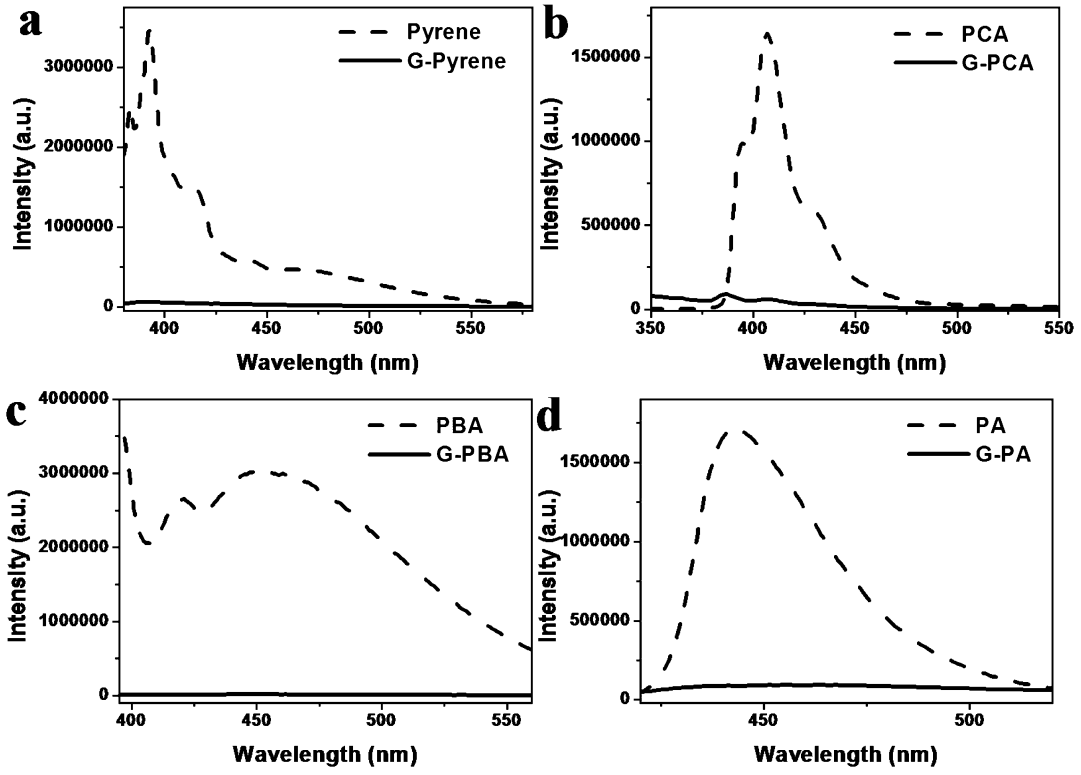

Figure 6. Fluorescence spectra of pyrene-derivatives and relevant graphene dispersion ((a) G-pyrene, (b) G-PCA, (c) G-PBA, and (d) G-PA) in DMF. Excitation wavelength: 356, 298, 373, and 398 nm for pyrene, PCA, PBA, and PA, respectively.

of its high specific surface area and excellent electrical conductivity.[48−50] In the following study, we prepared graphene/Au NPs composite. Because the original structure of the graphene is maintained, the performance of graphene/Au

dx.doi.org/10.1021/sc3000724 | ACS Sustainable Chem. Eng. 2013, 1, 144−151

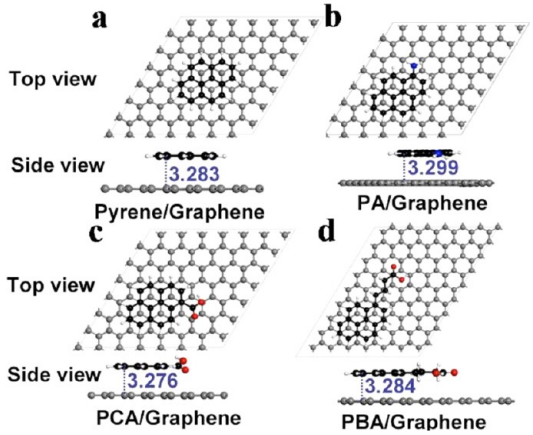

Figure 7. Optimized structures of (a) pyrene, (b) PA, (c) PCA, and (d) PBA on a single-layer graphene.

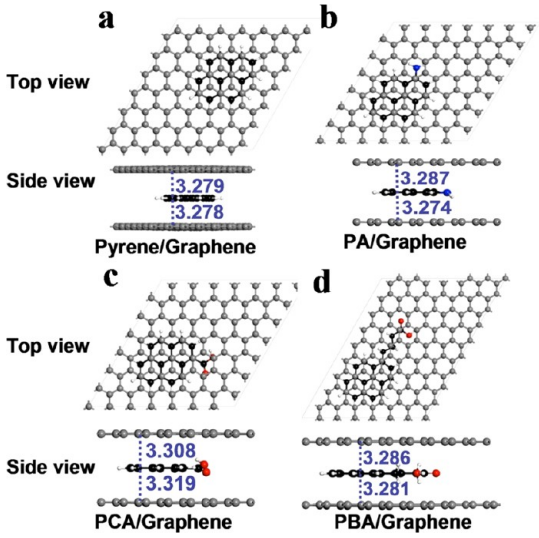

Figure 8. Optimized structures of (a) pyrene, (b) PA, (c) PCA, and (d) PBA between two graphene sheets.

Table 1. Interaction Energies of Graphene, Pyrene, PCA, PA, and PBA with Graphene Sheet Per Carbon Atom (IE_a, meV atom^{-1}) and between Two Graphene Sheets Per Carbon Atom (IE_b, meV atom^{-1}) Calculated with the vdW-Refined DFT

molecule		IE_a	ΔIE_a	IE_b
graphene	A−A stacking	−38.0		
	A−B stacking	−50.0		
pyrene		−62.0	−12.0	−155.0
PCA		−64.0	−14.0	−157.0
PA		−70.0	−20.0	−163.0
PBA		−71.4	−21.4	−172.0

NPs composite fabricated by our method will be better than GO/Au NPs or chemical converted graphene (CCG)/Au NPs composite.[51] Besides, the further modification of Au nanoparticles on the obtained graphene will provide direct evidence that using the method, exfoliation and modification of graphene can be achieved in one step. Here we synthesized pyrene-derivatives functionalized graphene/Au NPs composite through in-suit growth of Au nanoparticles. Figure 11 is the typical TEM images of the nanocomposite of graphene/Au NPs. From the fold edge of graphene sheet in Figure 11 d and e (marked by black arrow), it can be observed clearly that Au NPs uniformly distribute on the both sides of graphene sheet. The experimental results indicated that pyrene-derivatives have uniformly adsorbed on the graphene surface and acted as interlinkers to attach Au NPs on the surface of graphene.[52] This is the further evidence that using pyrene-derivatives can successfully exfoliate and modify grapheme with assistance of SC CO_2.

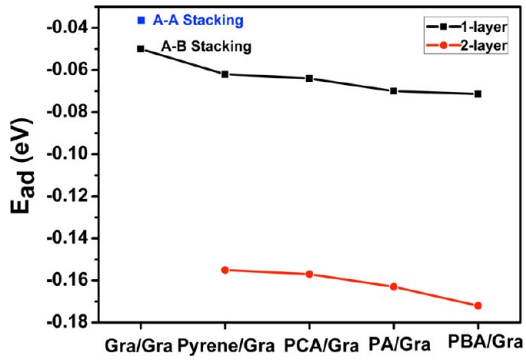

Figure 9. Interaction energies of graphene, pyrene, PCA, PA, and PBA with single-layer graphene per carbon atom and between two-layer graphene sheets per carbon atom.

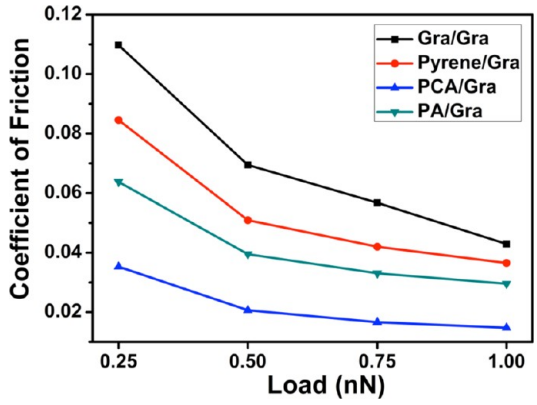

Figure 10. Coefficients of friction of pyrene, PA, and PCA with graphene and comparison with coefficients of friction of graphene dimers at different loads.

CONCLUSIONS

In summary, we have systematically studied the effect of pyrene and its derivatives (PCA, PBA, and PA) on the solvent-exfoliation graphene with the assistance of SC CO_2. Single or few layer high quality and noncovalent functionalized graphene were obtained in all cases. The high diffusivity and low viscosity of SC CO_2 facilitate the penetration and intercalation of pyrene-derivatives between the interlayer of graphite. On the basis of the vdW-refined DFT calculations, we identified the interaction of the pyrene-derivatives and graphene. The high interaction energies and low coefficients of friction between pyrene-derivatives and graphene indicate that pyrene-derivatives can act as a "molecular wedge" to exfoliate and modify graphene very well. In addition, we successfully prepared graphene/Au NPs composites. It indicates that obtained graphene modified with different pyrene-derivatives, will exhibit potential applications in sensors, catalysis, and microelectronic field in the future.

dx.doi.org/10.1021/sc3000724 | ACS Sustainable Chem. Eng. 2013, 1, 144−151

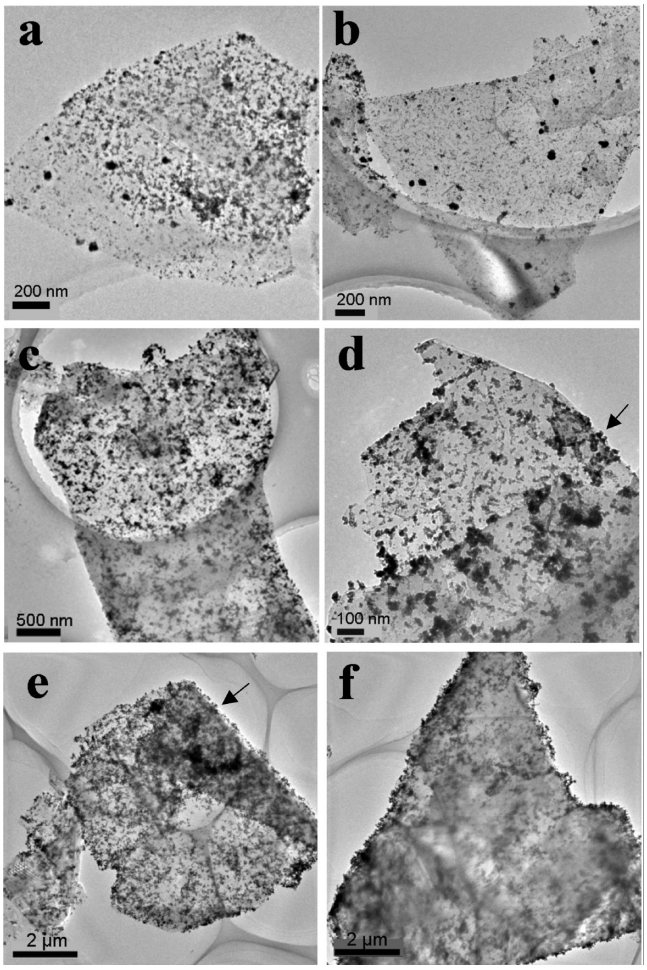

Figure 11. TEM images of G-PCA/Au NPs (a and b), G-PBA/Au NPs (c and d), and G-PA/Au NPs (e and f) composite.

AUTHOR INFORMATION

Corresponding Author

*E-mail: qunxu@zzu.edu.cn.

Notes

The authors declare no competing financial interest.

ACKNOWLEDGMENTS

We are grateful for the National Natural Science Foundation of China (Nos. 51173170, 50955010, and 20974102), Program for Excellent Scientist from Henan province (No. 114200510019), and the financial support from the Program for New Century Excellent Talents in University (NCET).

REFERENCES

(1) Novoselov, K. S.; Geim, A. K.; Morozov, S. V.; Jiang, D.; Zhang, Y.; Dubonos, S. V.; Grigorieva, I. V.; Firsov, A. A. Electric field effect in atomically thin carbon films. *Science* **2004**, *306*, 666−669.

(2) Geim, A. K.; Novoselov, K. S. The rise of graphene. *Nat. Mater.* **2007**, *6*, 183−191.

(3) Lee, C.; Wei, X.; Kysar, J. W.; Hone, J. Measurement of the elastic properties and intrinsic strength of monolayer graphene. *Science* **2008**, *321*, 385−388.

(4) Morozov, S.; Novoselov, K.; Katsnelson, M.; Schedin, F.; Elias, D.; Jaszczak, J.; Geim, A. K. Giant intrinsic carrier mobilities in graphene and its bilayer. *Phys. Rev. Lett.* **2008**, *100*, 016602.

(5) Balandin, A. A.; Ghosh, S.; Bao, W.; Calizo, I.; Teweldebrhan, D.; Miao, F.; Lau, C. N. Superior thermal conductivity of single-layer graphene. *Nano Lett.* **2008**, *8*, 902−907.

(6) Huang, X.; Qi, X.; Boey, F.; Zhang, H. Graphene-based composites. *Chem. Soc. Rev.* **2012**, *41*, 666.

(7) Zhu, Y.; Murali, S.; Cai, W.; Li, X.; Suk, J. W.; Potts, J. R.; Ruoff, R. S. Graphene and graphene oxide: Synthesis, properties, and applications. *Adv. Mater.* **2010**, *22*, 3906−3924.

(8) Huang, X.; Yin, Z.; Wu, S.; Qi, X.; He, Q.; Zhang, Q.; Yan, Q.; Boey, F.; Zhang, H. Graphene-based materials: Synthesis, characterization, properties, and applications. *Small* **2011**, *7*, 1876−1902.

(9) Huang, X.; Zeng, Z.; Fan, Z.; Liu, J.; Zhang, H. Graphene-based electrodes. *Adv. Mater.* **2012**, DOI: 10.1002/adma.201201587.

(10) He, Q.; Wu, S.; Yin, Z.; Zhang, H. Graphene-based electronic sensors. *Chem. Sci.* **2012**, *3*, 1764.

(11) Cui, X.; Zhang, C.; Hao, R.; Hou, Y. Liquid-phase exfoliation, functionalization and applications of graphene. *Nanoscale* **2011**, *3*, 2118−2126.

(12) Tung, V. C.; Allen, M. J.; Yang, Y.; Kaner, R. B. High-throughput solution processing of large-scale graphene. *Nat. Nanotechnol.* **2009**, *4*, 25−29.

(13) Hernandez, Y.; Nicolosi, V.; Lotya, M.; Blighe, F. M.; Sun, Z.; De, S.; McGovern, I. T.; Holland, B.; Byrne, M.; Gun'Ko, Y. K.; Boland, J. J.; Niraj, P.; Duesberg, G.; Krishnamurthy, S.; Goodhue, R.; Hutchison, J.; Scardaci, V.; Ferrari, A. C.; Coleman, J. N. High-yield production of graphene by liquid-phase exfoliation of graphite. *Nat. Nanotechnol.* **2008**, *3*, 563−568.

(14) Williams, G.; Seger, B.; Kamat, P. V. TiO_2-graphene nanocomposites. UV-assisted photocatalytic reduction of graphene oxide. *ACS Nano* **2008**, *2*, 1487−1491.

(15) Stankovich, S.; Piner, R. D.; Nguyen, S. T.; Ruoff, R. S. Synthesis and exfoliation of isocyanate-treated graphene oxide nanoplatelets. *Carbon* **2006**, *44*, 3342−3347.

(16) Xu, Y.; Bai, H.; Lu, G.; Li, C.; Shi, G. Flexible graphene films via the filtration of water-soluble noncovalent functionalized graphene sheets. *J. Am. Chem. Soc.* **2008**, *130*, 5856−5857.

(17) Liu, J.; Tang, J.; Gooding, J. J. Strategies for chemical modification of graphene and applications of chemically modified graphene. *J. Mater. Chem.* **2012**, *22*, 12435−12452.

(18) Qi, X.; Pu, K.-Y.; Zhou, X.; Li, H.; Liu, B.; Boey, F.; Huang, W.; Zhang, H. Conjugated-polyelectrolyte-functionalized reduced graphene oxide with excellent solubility and stability in polar solvents. *Small* **2010**, *6*, 663−669.

(19) Qi, X.; Pu, K.-Y.; Li, H.; Zhou, X.; Wu, S.; Fan, Q.-L.; Liu, B.; Boey, F.; Huang, W.; Zhang, H. Amphiphilic graphene composites. *Angew. Chem., Int. Ed.* **2010**, *49*, 9426−9429.

(20) Su, Q.; Pang, S.; Alijani, V.; Li, C.; Feng, X.; Müllen, K. Composites of graphene with large aromatic molecules. *Adv. Mater.* **2009**, *21*, 3191−3195.

(21) Zhang, M.; Parajuli, R. R.; Mastrogiovanni, D.; Dai, B.; Lo, P.; Cheung, W.; Brukh, R.; Chiu, P. L.; Zhou, T.; Liu, Z.; Garfunkel, E.; He, H. Production of graphene sheets by direct dispersion with aromatic healing agents. *Small* **2010**, *6*, 1100−1107.

(22) An, X.; Simmons, T.; Shah, R.; Wolfe, C.; Lewis, K. M.; Washington, M.; Nayak, S. K.; Talapatra, S.; Kar, S. Stable aqueous dispersions of noncovalently functionalized graphene from graphite and their multifunctional high-performance applications. *Nano Lett.* **2010**, *10*, 4295−4301.

(23) Li, X.; Zhang, G.; Bai, X.; Sun, X.; Wang, X.; Wang, E.; Dai, H. Highly conducting graphene sheets and Langmuir−Blodgett films. *Nat. Nanotechnol.* **2008**, *3*, 538−542.

(24) Zheng, J.; Di, C.-a.; Liu, Y.; Liu, H.; Guo, Y.; Du, C.; Wu, T.; Yu, G.; Zhu, D. High quality graphene with large flakes exfoliated by oleyl amine. *Chem. Commun.* **2010**, *46*, 5728−5730.

(25) Zeng, Z.; Yin, Z.; Huang, X.; Li, H.; He, Q.; Lu, G.; Boey, F.; Zhang, H. Single-layer semiconducting nanosheets: High-yield preparation and device fabrication. *Angew. Chem., Int. Ed.* **2011**, *50*, 11093−11097.

(26) Serhatkulu, G. K.; Dilek, C.; Gulari, E. Supercritical CO_2 intercalation of layered silicates. *J. Supercrit. Fluids* **2006**, *39*, 264−270.
(27) Rangappa, D.; Sone, K.; Wang, M.; Gautam, U. K.; Golberg, D.; Itoh, H.; Ichihara, M.; Honma, I. Rapid and direct conversion of graphite crystals into high-yielding, good-quality graphene by supercritical fluid exfoliation. *Chem.—Eur. J.* **2010**, *16*, 6488−6494.
(28) Horsch, S.; Serhatkulu, G.; Gulari, E.; Kannan, R. M. Supercritical CO_2 dispersion of nano-clays and clay/polymer nanocomposites. *Polymer* **2006**, *47*, 7485−7496.
(29) Li, J.; Xu, Q.; Peng, Q.; Pang, M.; He, S.; Zhu, C. Supercritical CO_2-assisted synthesis of polystyrene/clay nanocomposites via in situ intercalative polymerization. *J. Appl. Polym. Sci.* **2006**, *100*, 671−676.
(30) Pu, N.-W.; Wang, C.-A.; Sung, Y.; Liu, Y.-M.; Ger, M.-D. Production of few-layer graphene by supercritical CO_2 exfoliation of graphite. *Mater. Lett.* **2009**, *63*, 1987−1989.
(31) Miller, D. J.; Hawthorne, S. B.; Clifford, A. A.; Zhu, S. Solubility of polycyclic aromatic hydrocarbons in supercritical carbon dioxide from 313 to 523 K and pressures from 100 to 450 bar. *J. Chem. Eng. Data* **1996**, *41*, 779−786.
(32) Fifield, L. S.; Dalton, L. R.; Addleman, R. S.; Galhotra, R. A.; Engelhard, M. H.; Fryxell, G. E.; Aardahl, C. L. Noncovalent functionalization of carbon nanotubes with molecular anchors using supercritical fluids. *J. Phys. Chem. B* **2004**, *108*, 8737−8741.
(33) Kuo, C.-H.; Chiang, T.-F.; Chen, L.-J.; Huang, M. H. Synthesis of highly faceted pentagonal- and hexagonal-shaped gold nanoparticles with controlled sizes by sodium dodecyl sulfate. *Langmuir* **2004**, *20*, 7820−7824.
(34) Kresse, G.; Furthmüller, J. Efficient iterative schemes for ab initio total-energy calculations using a plane-wave basis set. *Phys. Rev. B* **1996**, *54*, 11169−11186.
(35) Kresse, G.; Joubert, D. From ultrasoft pseudopotentials to the projector augmented-wave method. *Phys. Rev. B* **1999**, *59*, 1758−1775.
(36) Perdew, J. P.; Burke, K.; Ernzerhof, M. Generalized gradient approximation made simple. *Phys. Rev. Lett.* **1996**, *77*, 3865−3868.
(37) Bučko, T. s.; Hafner, J. r.; Lebègue, S. b.; Ángyán, J. n. G. Improved description of the structure of molecular and layered crystals: Ab initio DFT calculations with van der waals corrections. *J. Phys. Chem. A* **2010**, *114*, 11814−11824.
(38) Monkhorst, H. J.; Pack, J. D. Special points for Brillouin-zone integrations. *Phys. Rev. B* **1976**, *13*, 5188−5192.
(39) Bang, G. S.; So, H.-M.; Lee, M. J.; Ahn, C. W. Preparation of graphene with few defects using expanded graphite and rose bengal. *J. Mater. Chem.* **2012**, *22*, 4806−4810.
(40) Ferrari, A. C.; Meyer, J. C.; Scardaci, V.; Casiraghi, C.; Lazzeri, M.; Mauri, F.; Piscanec, S.; Jiang, D.; Novoselov, K. S.; Roth, S.; Geim, A. K. Raman spectrum of graphene and graphene layers. *Phys. Rev. Lett.* **2006**, *97*, 187401.
(41) Gupta, A.; Chen, G.; Joshi, P.; Tadigadapa, S.; Eklund. Raman scattering from high-frequency phonons in supported *n*-graphene layer films. *Nano Lett.* **2006**, *6*, 2667−2673.
(42) Graf, D.; Molitor, F.; Ensslin, K.; Stampfer, C.; Jungen, A.; Hierold, C.; Wirtz, L. Spatially resolved raman spectroscopy of single- and few-layer graphene. *Nano Lett.* **2007**, *7*, 238−242.
(43) Liu, C.; Hu, G.; Gao, H. Preparation of few-layer and single-layer graphene by exfoliation of expandable graphite in supercritical *N*,*N*-dimethylformamide. *J. Supercrit. Fluids* **2012**, *63*, 99−104.
(44) Dreyer, D. R.; Murali, S.; Zhu, Y.; Ruoff, R. S.; Bielawski, C. W. Reduction of graphite oxide using alcohols. *J. Mater. Chem.* **2011**, *21*, 3443−3447.
(45) Chen, W.; Yan, L.; Bangal, P. R. Preparation of graphene by the rapid and mild thermal reduction of graphene oxide induced by microwaves. *Carbon* **2010**, *48*, 1146−1152.
(46) Yang, Q.; Pan, X.; Huang, F.; Li, K. Fabrication of high-concentration and stable aqueous suspensions of graphene nanosheets by noncovalent functionalization with lignin and cellulose derivatives. *J. Phys. Chem. C* **2010**, *114*, 3811−3816.
(47) Zacharia, R.; Ulbricht, H.; Hertel, T. Interlayer cohesive energy of graphite from thermal desorption of polyaromatic hydrocarbons. *Phys. Rev. B* **2004**, *69*, 155406.
(48) Bai, H.; Li, C.; Shi, G. Functional composite materials based on chemically converted graphene. *Adv. Mater.* **2011**, *23*, 1089−1115.
(49) Hong, W.; Bai, H.; Xu, Y.; Yao, Z.; Gu, Z.; Shi, G. Preparation of gold nanoparticle/graphene composites with controlled weight contents and their application in biosensors. *J. Phys. Chem. C* **2010**, *114*, 1822−1826.
(50) Huang, X.; Zhou, X.; Wu, S.; Wei, Y.; Qi, X.; Zhang, J.; Boey, F.; Zhang, H. Reduced graphene oxide-templated photochemical synthesis and in situ assembly of au nanodots to orderly patterned au nanodot chains. *Small* **2010**, *6*, 513−516.
(51) Goncalves, G.; Marques, P. A. A. P.; Granadeiro, C. M.; Nogueira, H. I. S.; Singh, M. K.; Grácio, J. Surface modification of graphene nanosheets with gold nanoparticles: The role of oxygen moieties at graphene surface on gold nucleation and growth. *Chem. Mater.* **2009**, *21*, 4796−4802.
(52) Ou, Y.-Y.; Huang, M. H. High-density assembly of gold nanoparticles on multiwalled carbon nanotubes using 1-pyrenemethylamine as interlinker. *J. Phys. Chem. B* **2006**, *110*, 2031−2036.